Progress in Valve Modeling at Stennis Space Center

R.L. Daines, J.L. Woods
Lockheed Martin Space Operations
Stennis Space Center, MS

P.R. Sulyma
NASA Stennis Space Center
Stennis Space Center, MS

ABSTRACT

The efforts to develop the capability to model valves used in testing rocket engine components at Stennis Space Center are documented. Both cryogenic liquid and gas valves models are presented. A 2-D model of a liquid valve yields reasonable agreement with experimental data for the valve flow coefficient. The numerical accuracy of the model is assessed. A 3-D pressure regulator valve model shows indications of the potential causes of unsteadiness observed during operation of the valve. Future directions for this work are noted.

INTRODUCTION

The ability to accurately model flow through valves and other test flow system elements is necessary to support the rocket engine and component testing that occurs at NASA Stennis Space Center. The present work details the efforts to build that capability, which will be useful for a variety of purposes. These include predicting valve behavior after a geometry modification or with a change in fluids. Fluids under cryogenic conditions can be sensitive to thermal and flow conditions. Other applications that are anticipated in the future include the valve design and design optimization to tailor valve trim sets to needs of test programs. Also, since testing requires ramping and changes in operating conditions during test, it is desirable to understand the transient behavior of valves.

This paper presents the work performed on two different valves: a cryogenic liquid control valve and a gas pressure regulator valve. The main objective of the cryogenic valve work was to use CFD to obtain an estimate of the valve flow coefficient as a function of valve plug position prior to testing a modified control valve. It was desirable to know what the valve coefficient curve would be like after the modification. In particular it was important to know from a control standpoint if there would be any areas of the flow curve that were not unique; that is, determine if there are multiple valve positions that would result in the same valve coefficient. The calculations were verified using grid sequencing studies and Richardson extrapolation, and the results were validated by comparison to subsequent experimental testing. The analysis allowed the visualization of flow phenomena occurring in the valve and an enhanced understanding of the valve behavior.

The modeled pressure regulator valve had been experiencing high-frequency chatter at high-flow conditions. It was desirable to understand the processes occurring in this valve and determine if

the unsteadiness could be flow induced.

The flows through the valves were modeled using the CFD code FDNS, developed at NASA Marshall Space Flight Center[1]. This code uses a pressure-based predictor-corrector algorithm that solves the governing equations for mass, momentum, and energy, along with a k–ε two-equation turbulence model with wall functions. The structured multi-block solver can operate in either serial or parallel mode.

RESULTS AND DISCUSSION

Liquid-Service Valve Modeling

Model setup The working fluid considered in the present effort is liquid nitrogen. The liquid nitrogen was assumed to be an incompressible liquid with a constant molecular viscosity. Properties of LN_2 at 162 R and 3000 psi were used. Because of lack of data, it was also assumed that the valve body was at the same temperature as the LN_2. This resulted in a flow with essentially a uniform temperature. At the inlet the mass flow rate was fixed. The exit boundary condition was set to conserve mass. All valve body or plug surfaces had to no-slip boundary conditions with constant wall temperatures applied. The centerline was treated as an axis of symmetry.

The geometry of this valve was assumed to be axisymmetric. For the plug and seat, this is exact, while for the rest of the valve it is an approximation. The assumed geometry up and downstream of the plug was modified to make it axisymmetric for the model. The area modeled started slightly upstream of the valve seat and extended about six duct diameters downstream, which is sufficient to allow the flow to realign with the duct and pressure to recover. Figure 1 shows a computational grid with the plug at the 45% open position consisting of about 16,000 points.

For the present task, 11 valve plug positions were modeled from 20% to 100% open. Experimental test data for seven valve plug positions was obtained after the modeling was done and was used for comparison to validate the computational results.

The results of the modeling were normalized by converting to a valve flow coefficient, C_v. To calculate C_v the integrated mass flow rate at the inlet and the difference of averaged pressures at the inlet and full pressure recovery point downstream of the plug were used

$$C_v = \frac{\dot{m}}{\sqrt{\Delta P}} \tag{1}$$

Verification of calculations Verification of the calculations performed for this task was done with a grid doubling study for the 65% open valve position. Three grids were generated with approximately 16,000, 60,000, and 230,000 grid points. These will be referred to as the "coarse", "medium", and "fine" grids respectively. Richardson Extrapolation was used to estimate the numerical error on each grid[2]. Using Richardson Extrapolation on the C_v values for these three grids, an order of convergence of 1.32 was determined for this class of problems using FDNS. This means that when the grid is doubled, the error is reduced by a factor of $2^{1.32} = 2.5$.

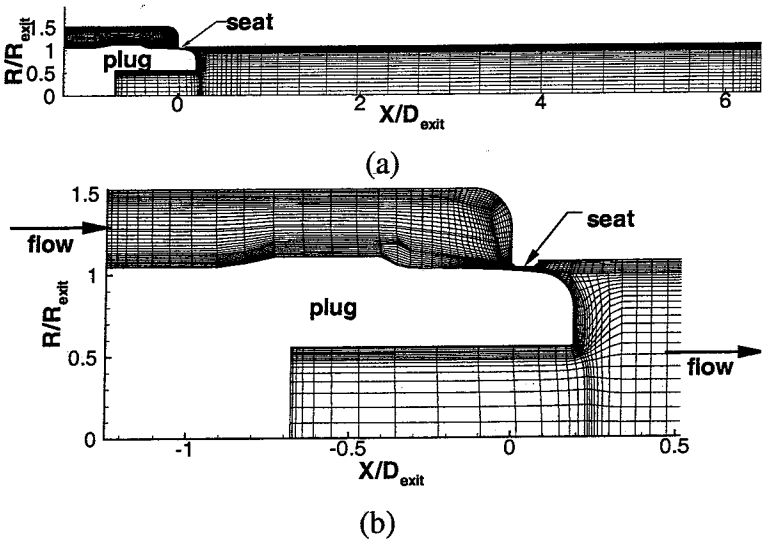

Figure 1: Typical grid for the cryogenic liquid control valve modeling effort. This grid is for the plug in the 45% open position. Every other grid point in each direction is removed for clarity. a) Overall geometry, b) close-up of the plug/seat region.

With the order of convergence calculated, error bands and an extrapolated grid-independent value for C_v could be calculated. The Grid Convergence Index (GCI) is an error band that bounds the maximum numerical error[2]. The extrapolated grid-independent value of C_v on the other hand is the predicted value that should be achieved on an infinitely fine grid. Both the extrapolated grid-independent value and the error bands on the calculated values of C_v are shown in Figure 2. As expected, refining the grid decreases the magnitude of the error bands and drives the value of C_v asymptotically toward the predicted grid-independent limiting value.

To test whether Richardson Extrapolation was accurate in predicting the asymptotic value of C_v, Richardson Extrapolation was applied to an "extra-fine" grid of around 900,000 points generated by grid doubling and the expected value of C_v was calculated. An FDNS solution was then obtained for this grid and C_v was determined from the results. The expected and computed values varied by less than 0.1%, giving confidence in the results yielded by the CFD verification process. With the validity of the extrapolation approach confirmed, five other valve positions were computed on "coarse" and "medium" grids and asymptotic values of C_v were determined.

Comparison to experiment Figure 3 shows the global results of this modeling effort in terms of C_v as a function of valve position for liquid nitrogen flow through the control valve. Modeled results from the eleven valve positions on "medium" density grids are shown as "+" symbols. Results from six of the plug positions utilized verification techniques and include the GCI numerical error bars. These GCI's range from 5.4% to 14.5%. Extrapolated grid-independent values from these cases are shown as circles. The other five calculated data points come from the initial set of grids generated which were not amenable to grid sequencing with the tools available at the time. It can be seen that the curve is smooth and monotonically increasing with increasing plug position. CFD results did not indicate any plug positions that would result in a smaller C_v than at a smaller valve

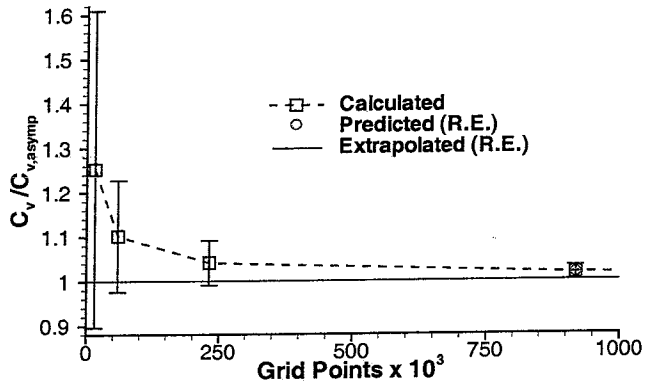

Figure 2: Calculated control valve C_v for different grid densities at a plug position of 65% open, showing the calculated numerical error bands for each point and the theoretical grid independent value of C_v from Richardson Extrapolation.

opening. This had been a concern going into the test program and would have caused a control problem if it had existed. The numerical results place the knee in the C_v curve at about 55% open.

Experimental test results are also shown in Figure 3 as squares for plug positions ranging from 9% to 68% open. It is noted that the experimental data point at 68% open, shown as an open symbol, is not considered well-characterized because of the small pressure drop at that position but is included to demonstrate the character of the C_v curve. Qualitatively, agreement between test data and modeled results is good. All trends are modeled correctly; testing confirmed the monotonic increase in C_v with increasing plug position. The test results place the knee in the C_v curve at about 58% open which agrees well with the calculated value. The valve model will need to be run at the plug positions used in the test to make direct comparisons between the test data and calculation. For full validation, error bars on the test data will also be required.

Besides global results, the CFD analyses also yielded flow details that aided in understanding the flow processes involved and how those processes changed as plug position changed. Understanding the flow behavior in relation to the minimum pressure point is beneficial to understanding the overall valve performance. The pressure drop in the region of the valve around the seat and plug for a range of plug positions is shown in Figure 4. At plug positions 55% open or less, a region of high pressure drop extends along the length of the seat and extends over the nose of the plug, with the greatest pressure drop occurring at the trailing corner of the upstream face of the seat. This corner corresponds to the minimum flow area for these configurations.

The character of the flow begins to change at 55% open. The trailing edge of the plug, which is more tapered, faces the seat at this plug location. The low pressure region no longer extends over the entire length of the seat as it does for smaller valve openings. It is noted that this plug position is the approximate location of the knee in the C_v curve. The pressure drop and corresponding losses at larger valve openings are considerably smaller. At 60% open the minimum pressure point is in the process of transitioning from the trailing edge to the leading edge of the upstream face of

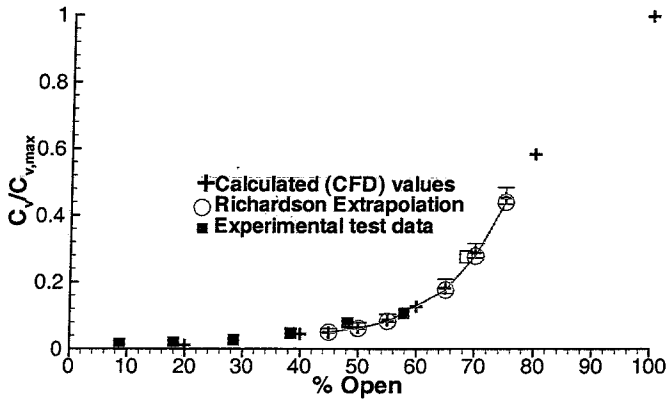

Figure 3: Valve coefficient C_v as a function of plug position for LN_2. Calculated, extrapolated, and experimental test values for the control valve are shown. Numerical error bars are shown on calculated values when available.

the seat. By 65% open, that transition is complete and the minimum pressure point is beginning to transition to the trailing nose of the plug. These transitions appear to be smooth and therefore do not cause an instability in the behavior of the valve, such as a local decrease in C_v with increasing plug location.

Streamlines and velocity magnitude for three plug positions are shown in Figure 5. The region of the valve near the valve seat and plug are shown, including the space in the center of the plug. The bottom of each figure is the centerline of the nozzle. The Coanda effect keeps flow attached to the nose of the plug and directs it toward the centerline of the valve. This creates a recirculation zone near the valve body immediately downstream of the seat over the entire range of plug positions. The separation point occurs at the downstream face of the valve seat. At 65% open, the separation point has begun to move forward on the seat toward the upstream face. In every case a recirculation zone also exists in the hollow core of the plug.

From the comparison with experimental results it is clear that the assumption of axisymmetry was acceptable. The computed results successfully captured the essential qualities of the experimental test data. There are three reasons for the success of this assumption in this case. First, C_v is a measure of the losses in the valve. The losses all occur near the seat and plug in this configuration. In the physical valve these areas are truly axisymmetric geometrically. Second, the fluid is accelerated in the axial direction by the narrowing flow passage as the flow enters the high-loss region. As this axial acceleration occurs, the radial and tangential components of velocity become less important, thus minimizing any effect of initially three-dimensional flow entering the seat/plug region. Third, as flow moves downstream after the end of the seat/plug region into a three-dimensional region of the valve, flow losses are negligible compared to the losses around the seat, so any three dimensionality of the flow is unimportant to C_v. These three characteristics of this valve make the axisymmetric assumption acceptable for the present analysis.

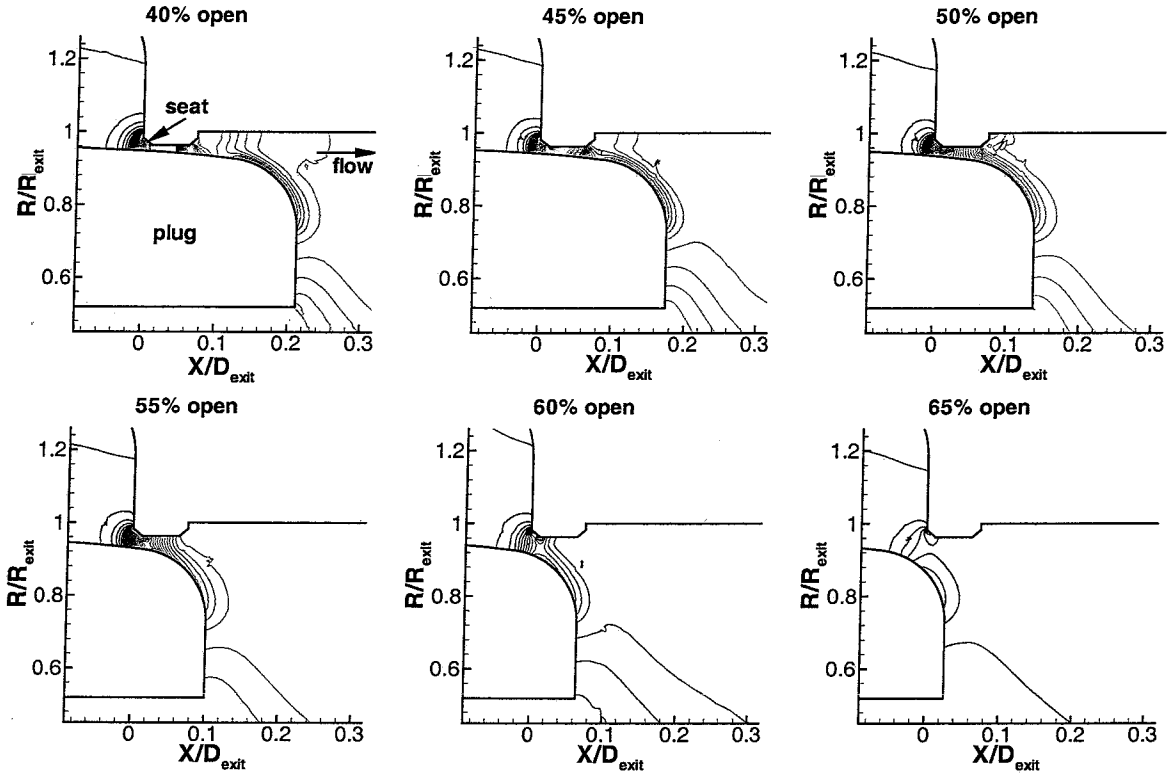

Figure 4: Normalized pressure contours near the control valve seat and plug for a range of plug positions. Red indicates greater pressure drop.

Gas-Service Valve Modeling

A gas pressure regulator valve analysis has also been performed. The motivation was to try to understand some observed unsteadiness in the operation of the valve. Three dimensionality was important to both the flow and geometry, so a full 3-D model was necessary. A schematic of the geometry is shown in Fig. 6. The grid that was used in the present analysis has approximately 500,000 grid points. Helium at ambient temperature was used as the working fluid. For the boundary conditions, the inlet stagnation pressure and exit static pressure were fixed.

The unsteady nature of this flow was captured qualitatively using a constant time step. The transient formulation of the code was not properly implemented at the time this work was performed, so quantitative results were not obtained. A time step of $0.1\mu s$ was used. Results presented here were obtained after the solution had become somewhat periodic.

Results from this modeling effort gave some indication of the nature of the unsteady flow phenomena that were likely to occur in this valve. The unsteadiness appeared to be related to the valve body geometry. A critical area for unsteadiness is in the area immediately downstream of the poppet. Figure 7 shows streamtraces over an interval time in the area the valve immediately downstream of the poppet. It can be seen that on the right side of the figure, which is the side of the valve toward the inlet pipe, that a large time varying recirculation zone has set up. The

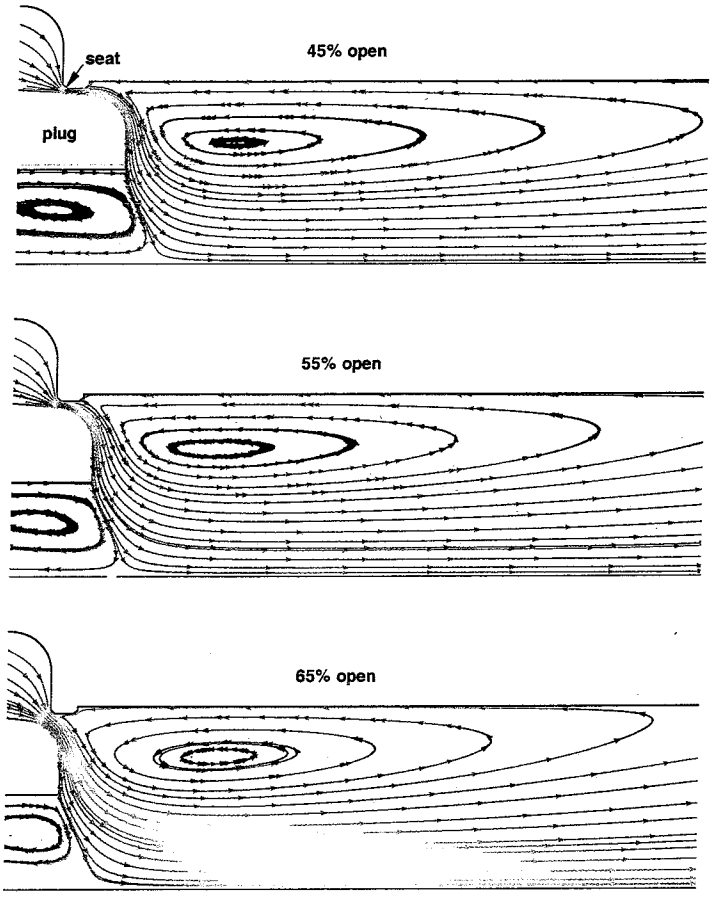

Figure 5: Streamlines for a range of plug positions in the control valve. Color indicates velocity magnitude, with red indicating higher velocities and blue indicating lower velocities.

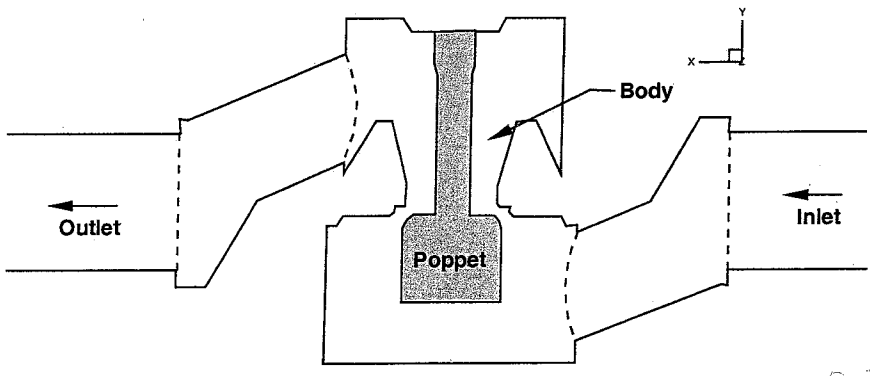

Figure 6: Schematic drawing of a cross-section of the pressure regulator valve showing the inlet, outlet, poppet, and body.

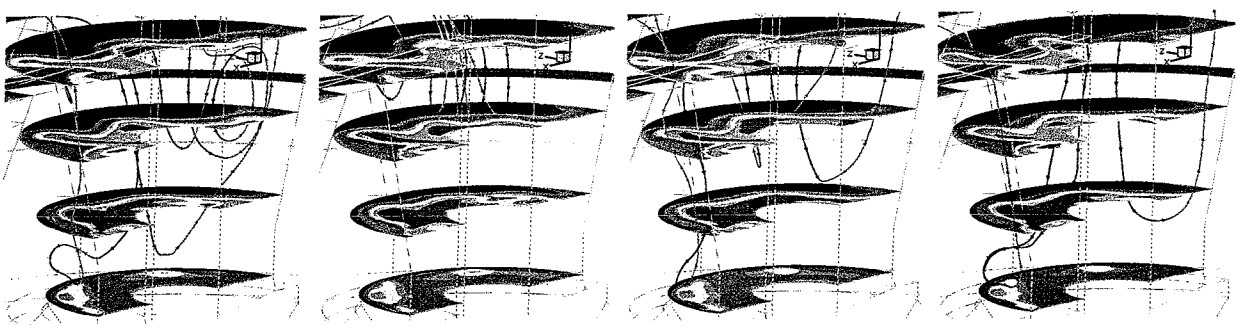

Figure 7: Velocity contours and streamtraces in the pressure regulator valve body over a period of time. Blue indicates downward (negative) velocities while red indicates the largest upward velocities. The bottom slice is located near the face of the poppet.

size of the recirculation zone varies, with reversed flow coming very close to the poppet when recirculation zone is a maximum size. Pressure contours at the poppet face in Fig. 8 indicate this recirculation zone is causing pressure fluctuations, primarily on the right half of the poppet face. Pressure fluctuations are on the order of 10 atm, with fluctuations as high as 40 atm in some areas. This changing pressure will results in a varying force from the gas on the poppet and could be a contributing cause to the chatter that is being experienced. Recirculation and swirl were also noted in the exit pipe. Unsteadiness from this region could be feeding upstream and influencing the flow in the main valve body.

Clearly to fully address this problem, full time-accuracy and the ability to model the poppet moving would be required. However, this preliminary investigation has given some indication of potential causes of the unsteadiness.

SUMMARY

Progress has been made toward routine modeling of both gas- and liquid-service valves at Stennis Space Center. Many the tools necessary to this effort are in place, and others are being obtained. An understanding of the behavior of cryogenic valves is progressing. The predictions for an axisymmetric model of a valve were verified and compared with experimental data. An initial investigation of the gas valve shows promise. It is recognized that an unstructured solver capability is necessary for the efficient modeling of complex geometries, especially for 3-D flowfields.

Future directions include modeling the full thermodynamic behavior of cryogenic fluids including the possibility of cavitation. Another area that will be important in the future is modeling transient flow in valves. Flow rates are strongly affected by the rate at which a valve is opened or closed; the steady-state valve coefficients typically do not represent flow rates and pressure drops when transient flows are occurring under component testing-type conditions. This is important since delivering propellants to the right places in the right amounts during start-up is a critical safety issue. By better understanding valve transients, we will be able to assist in providing a better testing environment for engine components. Finally, work is currently being done to develop the

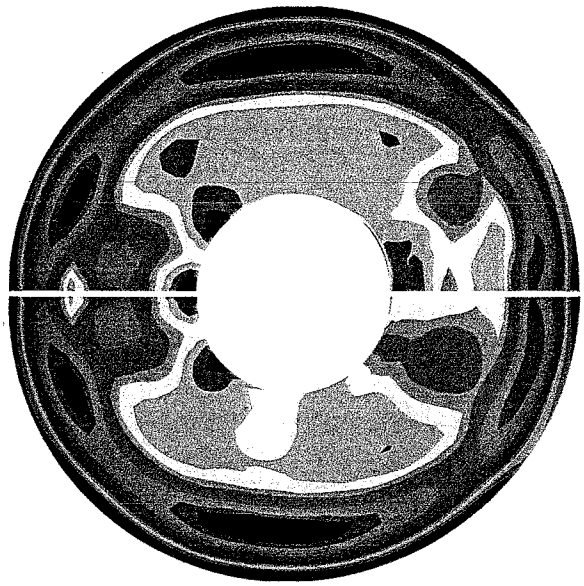

Figure 8: Pressure contours on the poppet face of the pressure regulator valve during a period of higher pressure (upper half) and lower pressure (lower half). Red indicates higher pressure.

capability to optimize valve designs, which will allow us to customize valve trim sets based on the conditions under which the valves will be used.

REFERENCES

[1] Chen, Y., "Compressible and Incompressible Flow Computations with a Pressure Based Method," AIAA Paper 89-0286, AIAA 27th Aerospace Sciences Meeting, Reno, NV, January 9-12 1989.

[2] Roach, P., *Verification and Validation in Computational Science and Engineering*, Hermosa Publishers, Albuqerque, NM, 1998.

REPORT DOCUMENTATION PAGE

Form Approved
OMB No. 0704-0188

1. REPORT DATE *(DD-MM-YYYY)*	2. REPORT TYPE	3. DATES COVERED *(From - To)*
04-12-2003		

4. TITLE AND SUBTITLE
Progress in Blave Modeling at SSC

5a. CONTRACT NUMBER
NAS13-650

5b. GRANT NUMBER

5c. PROGRAM ELEMENT NUMBER

6. AUTHOR(S)
Russell Daines
Jody Woods
Peter Sulyma

5d. PROJECT NUMBER

5e. TASK NUMBER

5f. WORK UNIT NUMBER

7. PERFORMING ORGANIZATION NAME(S) AND ADDRESS(ES)
LMSO - Space Programs

8. PERFORMING ORGANIZATION REPORT NUMBER
SE-2002-12-00080-SSC

9. SPONSORING/MONITORING AGENCY NAME(S) AND ADDRESS(ES)
Program Integration Office

10. SPONSORING/MONITOR'S ACRONYM(S)

11. SPONSORING/MONITORING REPORT NUMBER

12. DISTRIBUTION/AVAILABILITY STATEMENT
Publicly Available STI per form 1676

13. SUPPLEMENTARY NOTES
Conference - Penn State Propulsion Engineering Research Center 14th Annual Smposium on Propulsion December 2002

14. ABSTRACT

15. SUBJECT TERMS

16. SECURITY CLASSIFICATION OF:			17. LIMITATION OF ABSTRACT	18. NUMBER OF PAGES	19b. NAME OF RESPONSIBLE PERSON
a. REPORT	b. ABSTRACT	c. THIS PAGE			Russell Daines
					19b. TELEPHONE NUMBER *(Include area code)*
U	U	U	UU	9	(228) 688-3897